American Mineralogist, Volume 87, pages 1104–1112, 2002

Synthesis of beryllian sapphirine in the system MgO-BeO-Al_2O_3-SiO_2-H_2O and comparison with naturally occurring beryllian sapphirine and khmaralite. Part 1: Experiments, TEM, and XRD

A.G. CHRISTY,[1,*] Y. TABIRA,[2,†] A. HÖLSCHER,[3] E.S. GREW,[4] AND W. SCHREYER[3]

[1] Department of Applied Mathematics, Research School of Physical Sciences and Engineering, Australian National University, Canberra, ACT 0200, Australia

[2]Research School of Chemistry, Australian National University, Canberra, ACT 0200, Australia

[3] Institut für Geologie, Mineralogie und Geophysik, Ruhr-Universität Bochum, 44780 Bochum, Germany

[4] Department of Geological Sciences, University of Maine, 5790 Bryand Research Center, Orono, Maine 04469-5790, U.S.A.

ABSTRACT

Beryllian sapphirine $Mg_{4-x}Al_{4+x}[Al_{4+x-2y}Be_ySi_{2-x+y}O_{18}]O_2$ has been synthesized from starting compositions with $y \leq 1$ at $x = 0$ and $y \leq 0.5$ at $x = 0.5$, $P = 0.1$–1.3 GPa, $T = 700$–1350 °C. Electron diffraction shows the sapphirines are dominantly the 1*A* polytype but lamellae of a 2*M* phase are consistently present. This is the first 2*M* sapphirine synthesized in the laboratory, and the first known to be devoid of Fe^{2+}. No superstructure reflections corresponding to the doubled tetrahedral chain repeat of khmaralite were observed, probably due to insufficient annealing time. Cell parameters of the synthetic sapphirine decreased strongly and linearly with Be content (2.7 vol% decrease from $y = 0$ to $y = 1$). In agreement with crystal-chemical considerations, experiments with starting compositions of $y > 1.0$ resulted in additional crystalline phases either coexisting with the limiting sapphirine ($y = 1$) or without it. At 900 °C, 1.3–2.0 GPa, the saturating assemblage is surinamite + chrysoberyl + forsterite, which is chemically equivalent to sapphirine with $y = 1.5$. The current lack of natural khmaralite with Be > 0.78 cations per formula unit (pfu) is likely due to the bulk composition of the host rocks being too rich in SiO_2 and Al_2O_3 for forsterite to be stable. Addition of BeO to the MgO-Al_2O_3-SiO_2 system evidently enlarges the stability field of sapphirine + forsterite relative to its restricted range in the BeO-free system.

INTRODUCTION

The mineral sapphirine is a branched chain silicate with stoichiometry $M_8[T_6O_{18}]O_2$, in which the octahedral cations (M) are dominantly Al, Mg, and Fe^{2+} and the tetrahedral cations (T) are Al, Si, and Fe^{3+}. Less-common substituents include Ca and B (e.g., Grew et al. 1990, 1992), Ti (Harley and Christy 1995), and Be (e.g., Wilson and Hudson 1967; Grew 1981). The Be content ranges from near zero to 0.78 cations per 20 oxygen atoms; crystals with Be ≥ 0.5 cations per formula unit (pfu) show additional reflections in electron diffraction characteristic of the recently defined mineral species khmaralite (Barbier et al. 1999; Grew et al. 2000). Although originally found in silica-undersaturated metabasites of the granulite and amphibolite facies (cf., Deer et al. 1978 and references cited therein), sapphirine is now known from diverse high-grade metamorphic rocks, e.g., calc-silicate skarns (Jansen 1977; Grew et al. 1992) and quartzites (e.g., Ellis 1980; Grew 1980). There is also evidence that sapphirine may crystallize as a magmatic phase at high pressure (Liu and Presnall 1990, 2000; Harley and Christy 1995; Grew et al. 2000), and it may be widespread as a subsolidus reaction product in metabasites emplaced in the lower crust (Christy 1989a).

The major cations Mg, Al, and Si (with Fe^{2+} substituting for Mg, and Fe^{3+} for Al) show Tschermak's substitution (AlAl)$(MgSi)_{-1}$ within the approximate range $Mg_4Al_4[Al_4Si_2O_{18}]O_2$ ($2MgO{\cdot}2Al_2O_3{\cdot}SiO_2$ = the "2:2:1" composition) to $Mg_3Al_5[Al_5SiO_{18}]O_2$ ("3:5:1") (Fig. 1). The actual limits of the solution vary considerably as a function of pressure and temperature. Maximally silicic and magnesian sapphirines associated with enstatite can be very close to 2 Si per formula unit or near the "7:9:3" composition at the center of the range (Christy 1989b). Likewise, maximally aluminous sapphirines associated with spinel or aluminosilicates and corundum may be near the 7:9:3 composition (Sutherland and Coenraads 1996) or very close to 3:5:1 (minimum Si = 1.14 cations pfu; Godard and Mabit 1998).

The large, low-symmetry unit cell of sapphirine allows complex patterns of short- and long-range cation ordering. Despite some progress in characterization of the ordering through diffraction for aluminosilicate sapphirine (Moore 1969; Higgins and Ribbe 1979; Merlino 1980) and its gallogermanate analog

* Current Address: Department of Geology, Building 47, Australian National University, Canberra, ACT 0200, Australia. E-mail: agc110@rsphysse.anu.edu.au

† Current address: Materials Characterization Laboratory, Mitsui Mining and Smelting Co. Ltd., Corporate R&D Centre, Saitama-ken 362-0021, Japan.

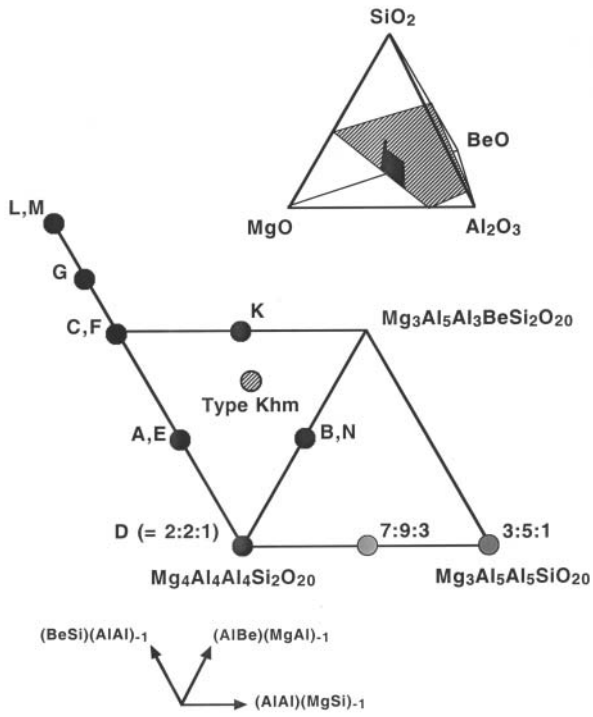

FIGURE 1. Location of sapphirine/khmaralite within the MBeAS tetrahedron, and compositions of starting mixtures used in this study (solid circles), 7:9:3 or $Mg_{3.5}Al_9Si_{1.5}O_{20}$ and 3:5:1 or $Mg_3Al_{10}SiO_{20}$ (gray), and type khmaralite (hachured). Details of compositions A–N are provided in Table 1.

(Barbier 1998), and spectroscopic study (Bancroft et al. 1968; Steffen et al. 1984; Christy et al. 1992), it is still poorly understood. The ordering behavior prevents the detailed modeling of sapphirine solid solutions in the MgO-Al_2O_3-SiO_2 system.

Sapphirine also shows polytypic structural variation. The commonest structure is the 2*M* polytype with a 14 Å **b** repeat. However, 7 Å-thick (010) structural slabs may translate to produce macroscopic volumes of a 1*A* form isotypic with aenigmatite, $Na_2Fe_5Ti[Si_6O_{18}]O_2$ (Cannillo et al. 1971; Merlino 1973), and microscopic intergrowths of 4*M* (Merlino and Pasero 1987), 3*A*, and 5*A* phases (Christy and Putnis 1988). Detailed study of nearly 30 natural and synthetic sapphirines showed that the 1*A* phase is stabilized by high pressure and low temperature (Christy 1989b). It was also the only polytype present in synthetic Fe-free (Christy 1989b) and Fe^{3+}-bearing sapphirines (Steffen et al. 1984), implying that the minor Fe^{2+} present in most natural sapphirines is essential for stabilization of the dominant 2*M* structure. Supporting evidence is provided by the nearly Fe-free composition of the only known very high temperature (>1000 °C) natural 1*A* sapphirine, from a magnesian granulite xenolith in a norite (Harley and Christy 1995), but no syntheses of 2*M* sapphirine by incorporation of Fe^{2+} have been reported to date.

Khmaralite is a recently recognized mineral species having the same structural topology as sapphirine but differing in that the tetrahedral chain length is doubled due to partial ordering of Be at certain sites (Barbier et al. 1999). Grew (1981) originally described this mineral as a beryllian sapphirine with an anomalously high Si content from a pegmatite in the ultrahigh-temperature metamorphic Napier Complex of Enderby Land, Antarctica. The doubled tetrahedral chain of khmaralite was first noted by Christy (1988) using transmission electron microscopy (TEM). Only the advent of area detectors allowed Barbier et al. (1999) to refine the structure using X-rays. In contrast to khmaralite, Be is fully ordered at one site in the beryllosilicate mineral associated with it: surinamite, $Mg_3Al_3[AlBeSi_3O_{15}]O$, which has been found at 7 localities worldwide (Baba et al. 2000). Its structure is polysomatically related to that of sapphirine (Moore and Araki 1983; Christy and Putnis 1988; Barbier 1996; Barbier et al. 2002).

Increasing use of the ion and electron microprobes, laser-ablation inductively coupled plasma mass spectroscopy, and single-crystal refinement to analyze the light elements Li, Be, and B has intensified research activity on systems containing these elements (e.g., Hawthorne et al. 1995; Grew 1996). It has been shown that the light elements are concentrated in certain rock-forming minerals and can have a major influence on their crystal structure and relations with other phases, e.g., Li in staurolite (Dutrow et al. 1986) and B in the vesuvianite-wiluite series (Groat et al. 1998).

Be-bearing sapphirine, cordierite, and surinamite were successfully synthesized at Bochum during a study of phase relations in the MgO-BeO-Al_2O_3-SiO_2-H_2O (MBeASH) system (Hölscher 1987); results on the latter two minerals have already been published (Hölscher et al. 1986; Hölscher and Schreyer 1989). As part of this research effort, inspired particularly by the identification of khmaralite as a new mineral and by the increasing attention given to light elements, we report the results of Hölscher (1987) on synthetic beryllian sapphirine and its implications for the role of Be in the stability and phase relations of sapphirine.

EXPERIMENTAL METHODS

In a reconnaissance study of the stability and compositional range of beryllian sapphirine in the MBeASH system, Hölscher (1987) carried out 23 runs from 0.1 to 2.0 GPa and 750 to 1350 °C at Bochum. She succeeded in synthesizing a beryllian sapphirine in 20 of these runs. The synthetics were prepared by annealing amorphous gel starting materials; most anneals were done under hydrothermal conditions, although some were nominally dry. Gel compositions corresponded to sapphirine with 3.5 or 4 Mg cations per 20 oxygen atoms, with 0, 0.5, 1, 1.25, or 1.5 Be cations substituted via the vector $(BeSi)(AlAl)_{-1}$ relative to Be-free compositions (Fig. 1).

The present paper reports a detailed study of sapphirine in the products of the 7 runs in which synthesis was most successful. These are reported in Table 1, along with data for some other runs whose products have important implications for the limits of Be incorporation into sapphirine/khmaralite. Examination with a scanning electron microscope (SEM) and subsequent powder X-ray diffraction (XRD) were used to characterize the phases present in the run products (Fig. 2). No sapphirine formed for Be = 1.5, where it was replaced by a surinamite-chrysoberyl-forsterite assemblage. Complete synthesis is as-

TABLE 1. Starting materials and run conditions for sapphirine synthesis experiments

Sample*	Ref.†	Starting composition per 20 O atoms ‡					*P* (GPa)	*T* (°C)	hours	Solid products§
		Mg	Al[6]	Al[4]	Be	Si				
A	IBS4a	4	4	3	0.5	2.5	0.5	1200	146	Spr; trace En, X in TEM
B	IBS4b	3.5	4.5	3.5	0.5	2	0.5	1200	146	Spr
C	IBS6	4	4	2	1	3	0.5	850	336	Spr
D	PBS7	4	4	4	0	2	1.3	900	112	Spr
E	PBS1a	4	4	3	0.5	2.5	1.3	900	42	Spr
F	PBS3a	4	4	2	1	3	1.3	900	67	Spr
G	PBS6	4	4	1.5	1.25	3.25	1.3	900	87	Spr, Sur, Cb, Fo
K	PBS3b	3.5	4.5	2.5	1	2.5	1.3	900	67	Spr, Cb, trace Crn?
L	PBS4	4	4	1	1.5	3.5	1.3	900	48	Sur, Cb, Fo
M	PBS5	4	4	1	1.5	3.5	2.0	900	94	Sur, Cb, Fo
N	PBS1b	3.5	4.5	3.5	0.5	2	1.3	900	42	Spr, trace Crn
–	PBS2a	4	4	3	0.5	2.5	1.3	750	89	Cb, Chl, Crn, trace Yod?
–	PBS2b	3.5	4.5	3.5	0.5	2	1.3	750	89	Spr, Crn
–	IBS2a	4	4	3	0.5	2.5	0.5	850	406	Spr
–	IBS2b	3.5	4.5	3.5	0.5	2	0.5	850	406	Spr, Crn

* Samples A–G were studied in detail in this paper.
† Sample reference number in Hölscher (1987).
‡ Water was added to all runs except for samples A and B.
§ Cb = chrysoberyl, Chl = Chlorite, Crn = corundum, En = enstatite, Fo = forsterite, Spr = sapphirine, Sur = surinamite, X = pseudohexagonal unknown, Yod = yoderite. Symbols after Kretz (1983).

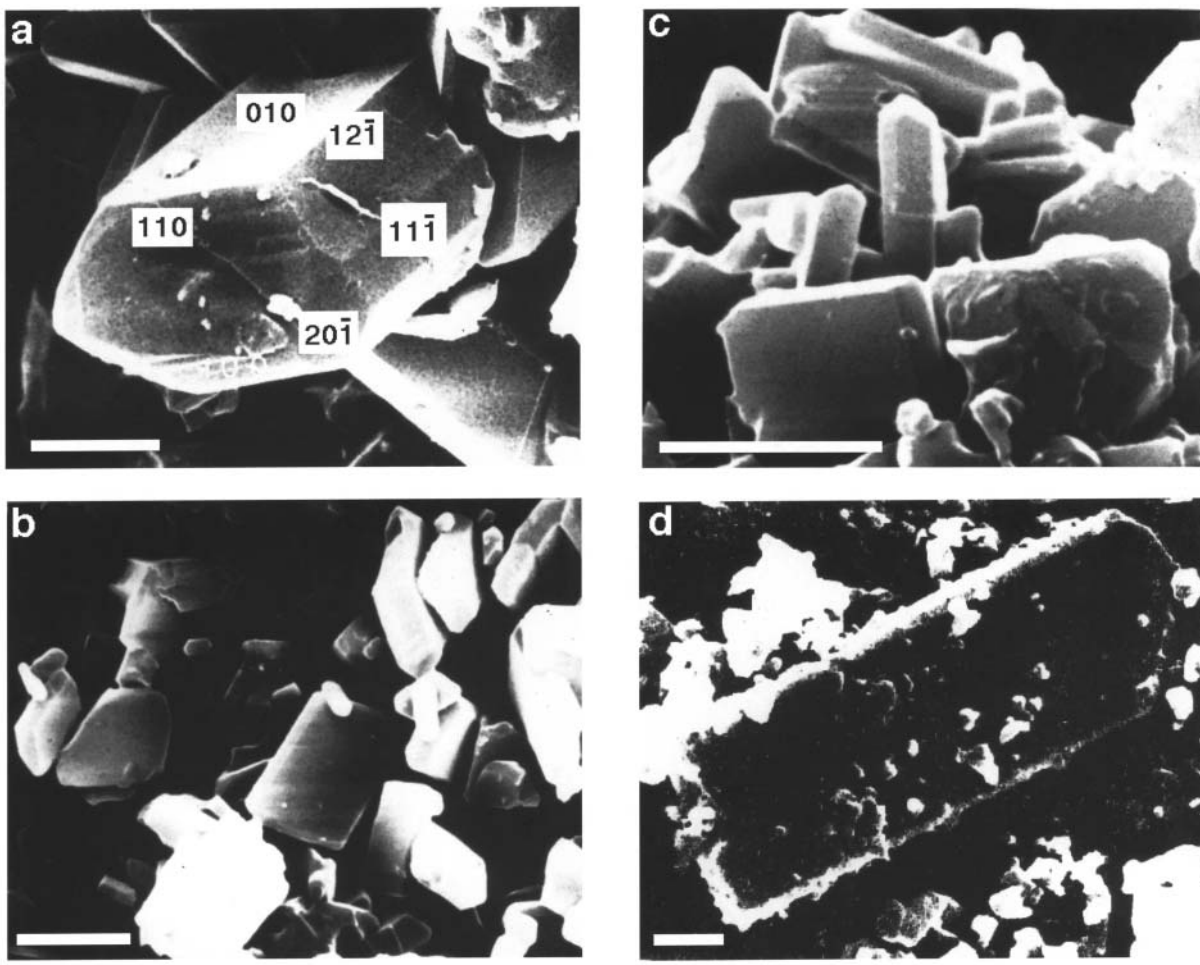

FIGURE 2. SEM micrographs of synthetic sapphirine crystals (from Hölscher 1987). Synthesis conditions for all were 1.3 GPa and 900 °C. SEM accelerating potential was 20 kV. White scale bar is 2 μm for all images. (**a**) Euhedral crystal with Be = 0 cations pfu (sample D). Face indices by analogy with morphological figure of Lacroix (1913) in Goldschmidt (1923), transformed onto unit cell of Moore (1969) according to the relationship in Sahama et al. (1974). (**b**) Be = 0.5 cations pfu (sample E). (**c**) Be = 0.5 cations pfu (sample E). (**d**) Be = 1.0 cations pfu (sample F).

sumed to imply that the sapphirine composition was very close to the initial gel stoichiometry. Three of these samples were examined by TEM in this study. These are labeled A–C in Table 1, which gives synthesis conditions. Hölscher (1987) refined unit-cell parameters for four additional samples that are listed as D–G in Table 1. Note that the nominal compositions of samples A and E are the same, as are those of C and F, although the synthesis pressures and temperatures are different for the members of each pair. Compositions of samples A, C, E–G are related to that of the 2:2:1 Be-free sapphirine (D) along the exchange vector $(BeSi)(AlAl)_{-1}$. The composition of sample B is similarly related to the 7:9:3 composition, and to the 2:2:1 composition along $(BeSi)(AlAl)_{-1} + (AlAl)(MgSi)_{-1} = (AlBe)(MgAl)_{-1}$ (Fig. 1): these are three of several vectors relating aenigmatite-group compositions (Burt 1994). All samples of this study were crystallized hydrothermally except A and B, which had no water added to the gel.

Powder XRD

Unit-cell parameters of samples A–C were obtained for this study by AGC using the 100 mm diameter, room-temperature Guinier powder X-ray camera at ANU. Cu$K\alpha_1$ radiation was used, and samples were ground together with NBS standard silicon 640a to provide an internal standard. The only optically visible impurities were some remnants of the Au capsule. A few very weak impurity lines were observed in the diffraction patterns.

Samples D–G were examined on a Siemens automated diffractometer at Bochum using Cu$K\alpha$ radiation (Hölscher 1987). Data were recorded over the range 10–74° 2θ.

Several axial settings have been used in the literature for the monoclinic and triclinic unit cells of sapphirine polytypes (Christy and Putnis 1988). Settings used in this paper are the $P2_1/a$ setting for sapphirine-2*M*, putting the tetrahedral chains of the structure parallel to **c** and in accordance with Higgins et al. (1979), Higgins and Ribbe (1979), Barbier and Hyde (1988), and Christy and Putnis (1988). This setting also was used in the first report of the khmaralite superstructure (Christy 1988) although not in the formal description of khmaralite as a new mineral (Barbier et al. 1999), where a $P2_1/c$ setting was used with $\beta \approx 90°$, which would correspond to a *B*-centered cell for sapphirine. The 1*A* cell used here is that of Merlino (1980). The two cells are related as follows:

$$\mathbf{a}_{1A} = \mathbf{c}_{2M}$$
$$\mathbf{b}_{1A} = {}^1/_2\mathbf{a}_{2M} - {}^1/_2\mathbf{b}_{2M} - {}^1/_4\mathbf{c}_{2M}$$
$$\mathbf{c}_{1A} = {}^1/_2\mathbf{a}_{2M} + {}^1/_2\mathbf{b}_{2M} + {}^1/_4\mathbf{c}_{2M}$$

TEM study

TEM study of samples A–C was conducted by Y.T. at the Electron Microscopy Unit, ANU, using a Phillips EM430 instrument. The accelerating potential was 300 kV, electron wavelength was 0.01969 Å, and the camera length was approximately 610 mm. Electron diffraction patterns and some images (none at high resolution) were recorded for many grains from all three samples.

Samples D–E were briefly examined on the JEOL 100 CX microscope at Cambridge (U.K.) by A.G.C. in 1988, using an accelerating voltage of 100 kV. A high-resolution pole piece and top-entry sample stage were used, which limited sample tilt to ±10° on two axes. The restricted tilt and small quantity of sample available prevented on-axis diffraction patterns and images being obtained, but some diagnostic off-axis patterns were recorded.

Diffraction patterns were identified and indexed using the Fortran program EDP3 written by A.G.C. This program accepts cell parameters, lattice type, and TEM parameters as interactive input, and lists zone axes in order of increasing lattice vector length, the radius of the corresponding first-order Laue zone (FOLZ) rings in the electron diffraction patterns, and four sets of *hkl* and *d** for each zone: the *hkl* indices for the two smallest independent *d** allowed by the lattice, and their vector sum and difference.

RESULTS

Powder XRD

Examination of the strong lines in the region 110–120° 2θ for samples A–C revealed no peak splitting due to departure from monoclinic symmetry. Fine intergrowth of 2*M* and 1*A* in two twin orientations evidently maintained the α and γ angles at 90° overall. Lines were relatively broad, which limited precision of position measurement to ±0.05 mm. The line width may have been a consequence of strain at twin boundaries and/or compositional heterogeneity. Interfacial strain in sapphirine should produce most line broadening for *hkl* reflections with large *k*. Lack of obvious orientation dependence suggests that inhomogeneity was the dominant factor.

From 26 to 34 reliably indexed line positions were used for refining 2*M* cell parameters using the program CELLP written by AGC. Estimated errors in cell edges were 0.004–0.008 Å (0.04–0.06%), which could not be improved by selecting more or less lines or differential weighting. Nevertheless, this precision is good enough to assess the relative effect of the exchange vectors $(AlAl)(MgSi)_{-1}$ and $(BeSi)(AlAl)_{-1}$ on molar volumes.

Powder XRD are presented in Table 2 for samples A-C, along with the data of Hölscher (1987) for samples D-G. The two data sets are consistent. Cell parameters and volume depend much more strongly on Be content than on Mg content. The cell parameters of the pairs with identical nominal compositions are the same to within 2 standard deviations.

The cell volumes for these sapphirines vary strongly and linearly with nominal Be content, as shown in Figure 3. Linear regression of the data for samples A and C–F gives $V_{cell} = 1320.19/\text{Å}^3 - 35.04x$ ($r = -0.997$), where x is the number of Be cations per 20 oxygen atoms. Data for sample B were excluded from the regression because it does not lie on the same $(BeSi)(AlAl)_{-1}$ line as the other beryllian sapphirines. However, it lies only 1.9 Å^3 below the line for the other samples, indicating that reduction of Mg content by the Tschermak vector $(AlAl)(MgSi)_{-1}$ causes only a small volume decrease. Data for G were excluded because synthesis was incomplete and hence the composition seemed uncertain at first. Nevertheless, the regression equation estimates Be as 1.01 cations per 20 oxygen atoms for this sample, effectively the same as for sample F. This finding implies that the maximum Be content of sapphirine with 4 Mg cations per 20 oxygen atoms is 1 at 900 °C, 1.3 GPa.

TABLE 2. Unit-cell parameters and cell volumes for samples of this study

	Be/20[O]	*a* (Å)	*b* (Å)	*c* (Å)	β (°)	*V* (Å³)
A	0.5	11.248 (5)	14.345 (8)	9.905 (5)	125.51 (3)	1301.0 (11)
B	0.5	11.254 (3)	14.338 (6)	9.905 (3)	125.53 (2)	1300.7 (8)
C	1.0	11.208 (4)	14.284 (8)	9.864 (4)	125.56 (3)	1284.7 (10)
D	0.0	11.282 (1)	14.441 (2)	9.956 (1)	125.49 (2)	1320.8 (2)
E	0.5	11.249 (1)	14.363 (2)	9.910 (1)	125.53 (1)	1303.1 (2)
F	1.0	11.216 (1)	14.291 (1)	9.868 (1)	125.61 (1)	1286.2 (1)
G	–	11.210 (2)	14.295 (3)	9. 862 (3)	125.62 (3)	1284.8 (4)
H*	–	11.18 (4)	14.26 (3)	9.82 (3)	125.1 (3)	1281 (7)
H'†	–	11.251 (8)	14.321 (12)	9.884 (16)	125.60 (6)	1294.9 (25)

* Povondra and Langer (1971).
† Re-indexed, this study.

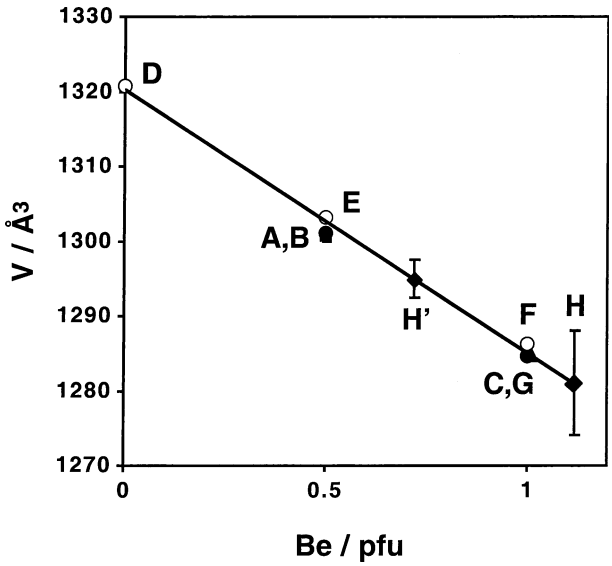

FIGURE 3. Unit-cell volumes of synthetic sapphirine as a function of Be content. Circles are samples A, C–F with volumes calculated from cell parameters obtained in this study (solid) or by Hölscher (1987, open). Other symbols indicate samples B (square), G (triangle), and H (diamonds). Sample H plotted with volume of Povondra and Langer (1971, H) and recalculated in this study (H'). Be contents of G, H, and H' were obtained from regression line fitted to A, C–F only.

A maximum Be content of 1.0 cations pfu appears to be in contradiction with data published for a beryllian sapphirine by Povondra and Langer (1971). Their material was produced by annealing of a devitrified glass of composition corresponding to an Na-, Be-bearing cordierite at 0.61 GPa, 1100 °C. The cell parameters given for this sapphirine, when transformed into the $P2_1/a$ setting, are: a = 11.18 (4) Å, b = 14.26 (3) Å, c = 9.82 (3) Å, β = 125.1 (4)°. The cell volume would correspond to 1.12 Be cations per 20 oxygen atoms according to the regression equation (Fig. 3). Sample, diffractometer traces, and refinement computer output were generously provided by Langer (Berlin) for re-examination. Although the remnant sample consisted largely of cordierite and contained too little sapphirine to give enough diffraction peaks for a new refinement, it was found that many of the strong peaks in the old diffractometer trace could be re-indexed so that more of them corresponded to sapphirine peaks that were expected to be strong. The new unit cell obtained using this indexing scheme had considerably lower estimated errors, a β angle more consistent with those of this study, and a larger cell volume consistent with a lower Be content of ca. 0.71 cations per 20 oxygen atoms. The two sets of cell data for this sample are labeled "H" (Povondra and Langer) and "H'" (this study) in Table 2 and Figure 3.

The dependence of cell volume on Be content for the sapphirines of this study is virtually identical to that of the natural Fe-bearing khmaralites and beryllian sapphirines described in Grew et al. (2000). A linear fit to their data gives V_{cell} = 1331.06 Å^3 – 36.46Be (r = –0.945).

Electron microscopy

Sapphirine was the only phase found in samples B–C and the dominant one in sample A (Table 1). One grain examined in sample A proved to be enstatite. Another grain gave a diffraction pattern unlike sapphirine or any of the expected impurity phases. Dimensions and geometry of the zero- and first-order Laue zones of the diffraction pattern implied a monoclinic unit cell with pseudohexagonal subcell, a = 7.86 Å, b = $2c_{hex}$ = 9.26 Å, c = $2a_{hex}$ = 15.73 Å, β = 120°. This material ("X" in Table 1) appears to be a new phase in the MBeASH system (Christy et al., in preparation).

All the observed sapphirine diffraction patterns were consistent with the 1*A* polytype being dominant. However, patterns that contained the $[1\bar{1}0]^*_{1A} = [010]^*_{2M}$ reciprocal lattice direction invariably showed strong streaking along this direction. Some patterns that did not contain this reciprocal direction also showed evidence of streaking: in the zero-order Laue zone (ZOLZ), *h* odd reflexions (1*A* axes) extended out to larger diffraction angles than *h* even reflexions, indicating that the *h* odd spots were more extended out of the plane of the ZOLZ. Patterns with beam direction $[uuw]_{1A}$ always showed the presence of both 1*A* twin orientations, but not usually in equal volume fractions. This result implies that the modal twin width was not significantly smaller than the diameter of the selected area aperture in the microscope, but was of the order of micrometers or larger. The majority of streaked patterns also showed weak additional maxima on the streaks halfway between 1*A* reflexions, which corresponded to minor amounts of the 2*M* polytype. The 2*M* reflections were elongated along the streak, which implies that the 2*M* phase existed only as narrow lamellae parallel to $(010)_{2M} = (1\bar{1}0)_{1A}$, in fully coherent intergrowth with 1*A* matrix (Fig. 4). Full coherence is usual for intergrowths of sapphirine polytypes (cf., Christy and Putnis 1988), but incoherent, misoriented intergrowths are also known when large lattice mismatches occur between polytypes. The mismatch in such cases is probably a consequence of compositional difference (Christy 1989b).

In the earlier study of samples D and E, heavily streaked 1*A* diffraction patterns were obtained, implying that this was the modally dominant polytype in these samples also. No evidence for discrete domains of the 2*M* phase was seen, although this may be due to the small amount of material available.

The superstructure reflections typical of khmaralite (Christy 1988, Barbier et al. 1999) were not observed for the sapphirines of this study (Fig. 5). No evidence was seen for non-conservative stacking faults of surinamite topology, as reported for Finero sapphirine by Christy and Putnis (1988). This result is

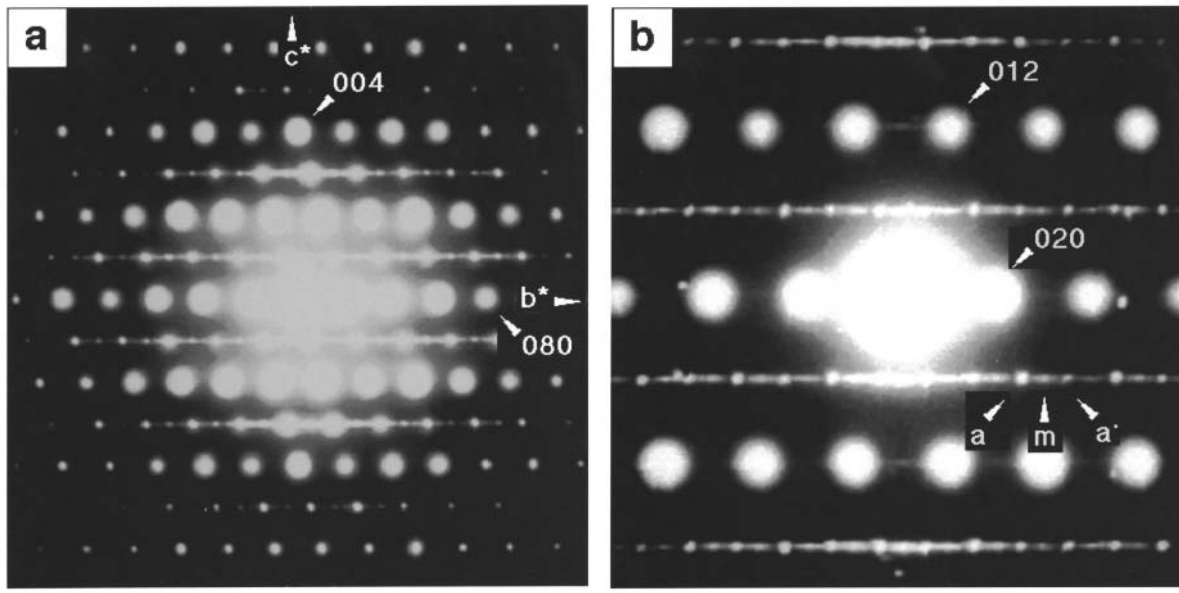

FIGURE 4. (**a**) $[100]_{2M}$ electron diffraction pattern from sample A, showing streaking parallel to **b*** with spots from the 2*M* and both twin orientations of 1*A* polytypes. (**b**) Magnified view of similarly oriented diffraction pattern from sample B. "m", "a," and "a'" indicate spots specific to 2*M* and the two orientations of 1*A* respectively. Miller indices are for 2*M* axes.

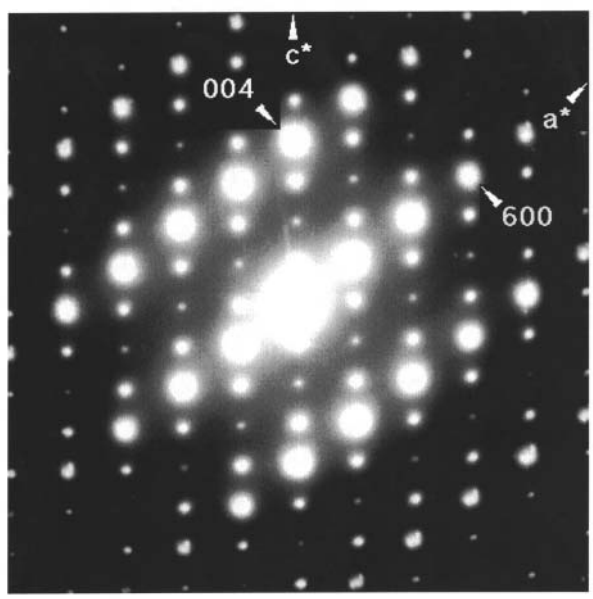

FIGURE 5. $[010]_{2M}$ diffraction pattern from sample C, showing no khmaralite superstructure spots (cf., Christy 1988).

consistent with such defects not being observed in TEM of natural khmaralite (Christy 1988; Barbier et al. 1999) despite the fact that macroscopic surinamite is an associated mineral (Grew 1981).

DISCUSSION

Polytypism and chain repeat

The elongated 2*M* diffraction spots observed in some electron diffraction patterns from samples A, B, and C are the first evidence that the 2*M* polytype of sapphirine can be synthesized. It is thus clear that Be substitution on the tetrahedral sites of sapphirine stabilizes the 2*M* polytype, as does Fe^{2+} substitution on the octahedral sites (Christy 1989b), and thus the 1*A* sapphirine/khmaralite polytype is not expected to be stable, except possibly at still higher pressures. It is not the small size of Be and Si relative to Al in the tetrahedral chain that achieves stabilization of 2*M* stacking, because the 1*A* structure predominates in Si-rich aenigmatite-group minerals related to sapphirine. Instead, relatively low bond strengths in the tetrahedral chain relative to the octahedral substructure may be important.

Grew et al. (2000) reported the occurrence of khmaralite superstructure spots for two samples with Be ≥ 0.5 cations per 20 oxygen atoms, and its absence for two samples with Be ≤ 0.5 cations. The lack of khmaralite superstructure spots in synthetic sapphirine with up to 1 Be cation pfu suggests that lower temperatures and/or long annealing times are required for tetrahedral ordering and the resulting superstructure reflections. Temperatures of original crystallization of natural khmaralite from anatectic pegmatitic melt could have approached the 1000–1100 °C, 0.9–1.1 GPa conditions estimated for metamorphism of the host rocks (e.g., Sandiford and Powell 1986; Harley 1998a, 1998b), i.e., conditions similiar to our experiments. However, khmaralite was affected by at least two metamorphic events subsequent to original crystallization: an earlier one at temperatures possibly as high as 800–900 °C and pressures approaching 0.8–0.9 GPa, and a later one at temperatures not exceeding 700 °C during decompression (Grew et al. 2000). Either event could have annealed what had originally crystallized as a beryllian sapphirine as disordered as the synthetic sapphirine, resulting thereby in khmaralite. In addition, the presence of substantial Fe, which is characteristic of natural khmaralite studied to date, may promote ordering of Be, a possibility suggested by clustering of Be and Fe in khmaralite

(Barbier et al. 1999). Ordering of Be, Al, and Si on tetrahedral sites increases with ordering of divalent and trivalent cations on octahedral sites in "makarochkinite," khmaralite, and surinamite (Barbier et al. 2001), suggesting the possibility of a mutual reinforcement during cation ordering.

Solid solution range of beryllian sapphirine as a function of *P*, *T* and composition

Figure 6 summarizes the full set of 23 experimental runs in Hölscher (1987), including partial and unsuccessful syntheses of sapphirine except one at 2.0 GPa, 900 °C. We emphasize that in these synthesis runs, no reactions were reversed and no products may be taken to represent true equilibrium. Nonetheless, we can use this diagram and Table 1 to draw some preliminary conclusions regarding the stability and compositional range of beryllian sapphirine.

(1) At $P \leq 0.2$ GPa, no synthesis for Be = 0.5 cations pfu yielded a product consisting only of sapphirine (Fig. 6). Instead, sapphirine was accompanied by chrysoberyl, magnesiotaaffeite-6*N*′3*S* ("taaffeite-9*R*" in Hölscher 1987; formerly "musgravite", see Armbruster 2002), spinel, cordierite, enstatite, mullite, and/or corundum (Table 1). Some of the assemblages were of variance too low to be at equilibrium. This result seems to indicate incomplete reaction due to slow kinetics at these low pressures. Because no cell parameters could be determined, composition of the sapphirine remains unknown.

(2) At 0.5 GPa, however, syntheses with Be = 0.5 cations pfu yielded single-phase sapphirine products at 1200 °C for Mg = 4 (sample A) and Mg = 3.5 (sample B). At 850 °C, single-phase sapphirine was obtained for Mg = 4 (sample C) but not for Mg = 3.5, which crystallized corundum as well (IBS2b, Table 1), suggesting that beryllian sapphirine with Mg <4 cations pfu is restricted to higher temperature.

(3) At 1.3 GPa and 900 °C, sapphirine syntheses were complete for Mg = 4, Be = 0.5 and 1 cations pfu (samples E-F), whereas runs at Mg = 3.5 gave Spr + Cb + trace Crn at Be = 1 (K, Table 1) and Spr + trace Crn at Be = 0.5 (N, Table 1). That is, sapphirine synthesis was complete at T = 850–900 °C only when Mg = 4; higher temperatures are required for complete synthesis at Mg = 3.5. Comparison with the runs at 850 °C, 0.5 GPa suggests that pressure has little effect on the extent of the Tschermak substitution.

(4) The maximum Be content observed in complete syntheses was 1.0 Be cation pfu At 1.3 GPa, 900 C and also at 2.0 GPa, 900 °C, synthesis attempts with Mg = 4, Be = 1.5 produced only surinamite + forsterite + chrysoberyl (L and M, Table 1), i.e., $Mg_4Al_5Be_{1.5}Si_{3.5}O_{20}$ = Sur + 0.5 Fo + 0.5 Cb (Fig. 7). This compositional degeneracy implies that the Be content

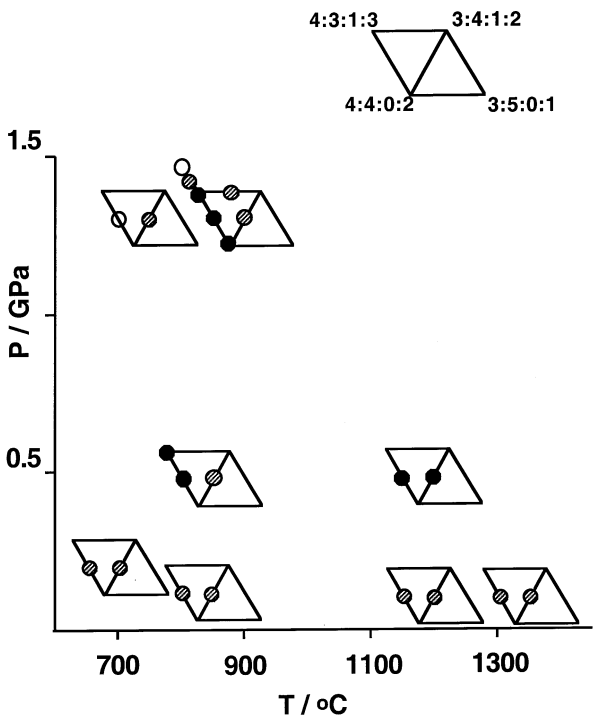

FIGURE 6. Pressures, temperatures, starting materials, and results of synthesis runs by Hölscher (1987). Circles indicate compositions of gels that gave complete sapphirine synthesis (solid), partial synthesis (hatched), or no sapphirine (open). Compositions at top right expressed as $MgO:Al_2O_3:BeO:SiO_2$.

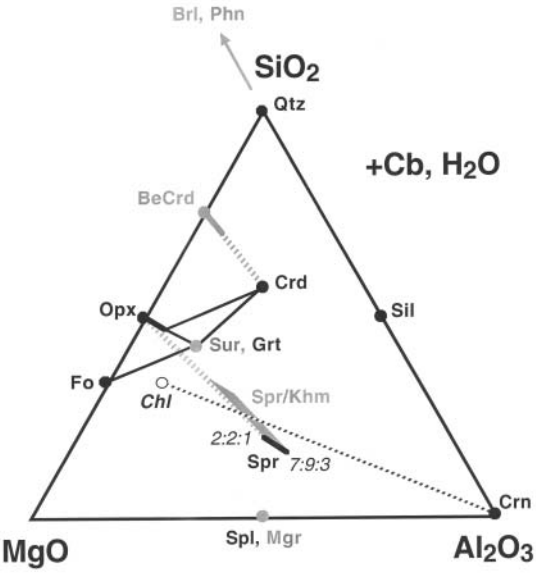

FIGURE 7. Phase compositions projected onto the MgO-Al_2O_3-SiO_2 plane from water and chrysoberyl, $BeAl_2O_4$ = Cb, which may coexist with all phases and assemblages under consideration. Solid symbols and lettering indicate absence of Be, gray symbols and lettering indicate presence of Be, or that Be-bearing phase is superposed on Be-free phase. Italicized label and open circle indicate chlorite (Chl) of clinochlore composition $[Mg_5Al_2Si_3O_{10}(OH)_8]$. Spr/Khm quadrilateral is defined by lines Mg = 4 (left) and Mg = 3.5 (right), Be = 0 (bottom) and Be = 1 (top). The hachured gray line extending from 2:2:1 sapphirine composition shows a hypothetical extrapolation of Spr/Khm solid solution beyond Mg = 4, Be = 1 toward the Mg = 4, Be = 2 composition, which plots at Opx. The other hachured line bridges the solvus gap between Crd and BeCrd. The dashed Chl-Crn line and solid Sur-Fo line are shown to illustrate limits imposed upon Spr/Khm solid solution by these assemblages under conditions where they are stable with Cb. Also shown are the joins Sur-Opx, Opx-Crd, and Sur-Crd that isolate Spr/Khm from high-Be phases such as BeCrd, beryl (Brl), and phenakite (Phn) in the presence of Cb.

of Spr/Khm must remain less than 1.5 Be cations pfu when (Sur + Fo + Cb) is stable. Because the starting material with 1.25 Be cations pfu (G, Table 1) yielded the same assemblage plus sapphirine, the true maximum Be at 1.3 GPa, 900 °C is evidently lower. Powder XRD data indicated 1.0 Be cations pfu (Table 2, Fig. 3).

(5) Sapphirine was synthesized with corundum at 750 °C, 1.3 GPa, i.e., 30 °C outside its stability field in the MASH system determined by Ackermand et al. (1975), suggesting that Be could lower the minimum temperature limit for sapphirine in the presence of water. However, sapphirine crystallized only in a gel with Mg = 3.5, Be = 0.5; for Mg = 4 at this Be content, Crn + Cb + chlorite (Chl) was found instead (Table 1). Coexisting (Chl + Cb + Crn) define a plane in the MBeAS tetrahedron that restricts sapphirine Be content to 0.4 cations pfu for Mg = 4 and to 0.6 cations pfu for Mg = 3.5 (Fig. 7). Assuming clinochlore, $Mg_5Al_2Si_3O_{10}(OH)_8$, as the most appropriate composition for chlorite, we can write the reactions 0.8 Chl + 2.4 Crn + 0.4 Cb = 3.2 H_2O + $Mg_4Al_{7.2}Be_{0.4}Si_{2.4}O_{20}$ and 0.7 Chl + 2.6 Crn + 0.6 Cb = 2.8 H_2O + $Mg_{3.5}Al_{7.8}Be_{0.6}Si_{2.1}O_{20}$. Therefore, under wet conditions and in the presence of the assemblage (Chl + Crn + Cb), maximum Spr Be content is much lower than in the anhydrous system.

In summary, these results and the re-examined data of Povondra and Langer (1971) give a maximum Be content of 1.0 Be cations per 20 oxygen atoms for Mg = 4 and below 1 for lower Mg contents. A maximum of 1 Be cation is consistent with the presence of a winged tetrahedral chain in which Be is strongly fractionated into tetrahedra with three bridging oxygen atoms (e.g., khmaralite, Barbier et al. 1999). In this chain, which is also found in aenigmatite-group minerals, two such sites share a corner, and both sites of this pair cannot be simultaneously occupied by Be without substantial underbonding of the bridging oxygen atom, i.e., only 1 Be cation per 6T sites can be incorporated. A possible exception is the aenigmatite-group mineral welshite, e.g., $Ca_2Mg_{3.8}Mn^{2+}_{0.6}Fe^{2+}_{0.1}Sb^{5+}_{1.5}O_2$ $[Si_{2.8}Be_{1.7}Fe^{3+}_{0.65}Al_{0.7}As_{0.17}O_{18}]$ (Moore 1978, Grew et al. 2001), but a full-scale refinement of its structure is needed to determine how the critical bridging oxygen atom is bonded.

The presence of Be in sapphirine appears to have a marked effect on the compatibility relationships of Spr with other phases, notably forsterite. In the pure MAS system, Spr + Fo has at most a small stability field at T << 800 °C and P < 0.5 GPa (cf., Grew et al. 1994), whereas in the syntheses of Hölscher (1987), the assemblage (Sur + Fo + Cb) occurs with or replaces highly beryllian Spr/Khm at T = 900 °C and P up to 2.0 GPa (Table 1). Under conditions where (Sur + Cb + Fo) is not stable, Spr/Khm might be found in association with other beryllian phases such as phenakite (Phn: Be_2SiO_4), beryl (Brl: ideally $Al_2Be_3Si_6O_{18}$), or the Be-cordierite (BeCrd: $Mg_2Al_2BeSi_6O_{18}$) of Hölscher and Schreyer (1989). However, the stability of assemblages such as (Opx + Sur + Cb), (Opx + Crd + Cb), and (Sur + Crd + Cb) would render these phases incompatible with Spr/Khm as well (Fig. 7). The only current evidence for the possible stability of Spr + Phn is one attempted synthesis of Sur by Hölscher et al. (1986) at 1 bar pressure and 1040 °C, which produced (Spr + Fo + Sil + Crd + Phn) instead. Pressure-temperature-composition behavior of Spr/Khm and a provisional MBeAS petrogenetic grid are discussed in more detail in part 2 of this study (Christy and Grew in prep.).

ACKNOWLEDGMENTS

We thank K. Langer for his kind provision of beryllian sapphirine samples and diffraction data. E.S.G.'s research was supported by United States National Science Foundation grant OPP-9813569 and OPP-0087235 to the University of Maine. A.G.C. acknowledges receipt of a visiting fellowship from the Research School of Chemistry, ANU. We thank John Dalton and John Schumacher for their helpful reviews of an earlier draft of this manuscript.

REFERENCES CITED

Ackermand, D., Seifert, F., and Schreyer, W. (1975) Instability of sapphirine at high pressures. Contributions to Mineralogy and Petrology, 50, 79–82.

Armbruster, T. (2002) Revised nomenclature of högbomite, nigerite, and taaffeite minerals. European Journal of Mineralogy, 14, 389–396.

Baba, S., Grew, E.S., Shearer, C.K., and Sheraton, J.W. (2000) Surinamite, a high-temperature metamorphic beryllosilicate, from Lewisian sapphirine-bearing kyanite-orthopyroxene-quartz-K-feldspar gneiss at South Harris, NW Scotland. American Mineralogist, 85, 1474–1484.

Bancroft, G.M., Burns, R.G., and Stone, A.J. (1968) Application of the Mössbauer effect to silicate mineralogy II: Fe silicates of unknown and complex structures. Geochimica et Cosmochimica Acta, 32, 547–559.

Barbier, J. (1996) Surinamite analogs in the MgO-Ga_2O_3-GeO_2 and MgO-Al_2O_3-GeO_2 systems. Physics and Chemistry of Minerals, 23, 151–156.

———(1998) Crystal structures of sapphirine and surinamite analogs in the MgO-Ga_2O_3-GeO_2 system. European Journal of Mineralogy, 10, 1283–1293.

Barbier, J. and Hyde, B.G. (1988) Structure of sapphirine: its relation to the spinel, clinopyroxene and beta-gallia structures. Acta Crystallographica, B44, 373–377.

Barbier, J., Grew, E.S., Moore, P.B., and Su, S.-C. (1999) Khmaralite, a new beryllium-bearing mineral related to sapphirine: A superstructure resulting from partial ordering of Be, Al and Si on tetrahedral sites. American Mineralogist, 84, 1650–1660.

Barbier, J., Grew, E.S., Yates, M.G., and Shearer, C.K. (2001) Beryllium minerals related to aenigmatite. Geological Association of Canada, Mineralogical Association of Canada, Joint Annual Meeting Abstracts, 26, 7.

Barbier, J., Grew, E.S., Hålenius, E., Hålenius, U., and Yates, M.G. (2002) The role of iron and cation order in the crystal chemistry of surinamite, $(Mg,Fe^{2+})_3(Al,Fe^{3+})_3O[AlBeSi_3O_{15}]$: A crystal structure, Mössbauer spectroscopic, and optical spectroscopic study. American Mineralogist, 87, 501–513.

Burt, D.M. (1994) Vector representation of some mineral compositions in the aenigmatite group, with special reference to høgtuvaite. Canadian Mineralogist, 32, 449–457.

Cannillo, E., Mazzi, F., Fang J.H., Robinson P.D., and Ohya, Y. (1971) The crystal structure of aenigmatite. American Mineralogist, 56, 427–446.

Christy, A.G. (1988) A new 2c superstructure in beryllian sapphirine from Casey Bay, Enderby Land, Antarctica. American Mineralogist, 73, 1134–1137.

———(1989a) The stability of sapphirine+clinopyroxene: implications for phase relations in the CaO-MgO-Al_2O_3-SiO_2 system under deep-crustal and upper mantle conditions. Contributions to Mineralogy and Petrology, 102, 422–428.

———(1989b) The effect of composition, temperature and pressure on the stability of the 1Tc and 2M polytypes of sapphirine. Contributions to Mineralogy and Petrology, 103, 203–215

Christy, A.G. and Putnis, A. (1988) Planar and line defects in the sapphirine polytypes. Physics and Chemistry of Minerals, 15, 548–558.

Christy, A.G., Phillips, B.L., Güttler, B.K. and Kirkpatrick, R.J. (1992) A ^{27}Al and ^{29}Si MAS NMR and infrared spectroscopic study of Al-Si ordering in natural and synthetic sapphirine. American Mineralogist, 77, 8–18.

Deer, W.A., Howie, R.A., and Zussmann, J. (1978) The Rock-Forming Minerals volume 2A: Single-Chain Silicates, 2nd edition. Longman, London.

Dutrow, B.L., Holdaway, M.J., and Hinton, R.W. (1986) Lithium in staurolite and its petrologic significance. Contributions to Mineralogy and Petrology, 94, 496–506.

Ellis, D.J. (1980) Osumilite-sapphirine-quartz granulites from Enderby Land, Antarctica: P-T conditions of metamorphism, implications for garnet-cordierite equilibria and the evolution of the deep crust. Contributions to Mineralogy and Petrology, 74, 201–210.

Godard, G. and Mabit, L.-J. (1998) Peraluminous sapphirine formed during retrogression of a kyanite-bearing eclogite from Pays de Léon, Armorican Massif, France. Lithos, 43, 15–29.

Goldschmidt, V.M. (1923) Atlas der Krystallformen, volume 8. Carl Winters Universitätsbuchhandlung, Heidelberg (in German).

Grew, E.S. (1980) Sapphirine + quartz association from Archean rocks in Enderby Land, Antarctica. American Mineralogist, 65, 821–836.

———(1981) Surinamite, taaffeite and beryllian sapphirine from pegmatites in granulite-facies rocks. of Casey Bay, Enderby Land, Antarctica. American Min-

eralogist, 66, 1022–1033.

———(1996) Borosilicates (exclusive of tourmaline) and Boron in rock-forming minerals in metamorphic environments. In E.S. Grew and L.M. Anovitz, Eds., Boron: Mineralogy, Petrology, and Geochemistry, 33, 387–502. Reviews in Mineralogy, Mineralogical Society of America, Washington, D.C.

Grew, E.S., Chernosky J.V., Werding G., Abraham K., Marquez N., and Hinthorne, J.R. (1990) Chemistry of kornerupine and associated minerals, a wet chemical, ion microprobe, and X-ray study emphasizing Li, Be, B and F contents. Journal of Petrology, 31, 1025–1070.

Grew, E.S., Yates, M.G., Romanenko, I.M., Christy, A.G., and Swihart, G.H. (1992) Calcian, borian sapphirine from the serendibite deposit at Johnsburg, NY, USA. European Journal of Mineralogy, 4, 475–485.

Grew, E.S., Pertsev, N.N., Yates, M.G., Christy, A.G., Marquez, N., and Chernosky, J. (1994) Sapphirine + forsterite and sapphirine + humite-group minerals in an ultra-magnesian lens from Kuhi-Lal, SW Pamirs, Tajikistan: Are these assemblages forbidden? Journal of Petrology, 35, 1275–1293.

Grew, E.S., Yates, M.G., Barbier, J., Shearer, C.K., Sheraton, J.W., Shiraishi, K. and Motoyoshi, Y. (2000) Granulite-facies beryllium pegmatites in the Napier Complex in Khmara and Amundsen Bays, western Enderby Land, East Antarctica. Polar Geoscience 13, 1–40.

Grew, E.S., Hålenius, U., Kritikos, M., and Shearer, C. K. (2001) New data on welshite, e.g., $Ca_2Mg_{3.8}Mn^{2+}_{0.6}Fe^{2+}_{0.1}Sb^{5+}_{1.5}O_2[Si_{2.8}Be_{1.7}Fe^{3+}_{0.65}Al_{0.7}As^{5+}_{0.17}O_{18}]$, an aenigmatite-group mineral. Mineralogical Magazine, 65, 665–674.

Groat, L.A., Hawthorne, F.C., Ercit, T.S., and Grice, J.D. (1998) Wiluite, $Ca_{19}(Al, Mg, Fe, Ti)_{13}(B,Al,\square)_5Si_{18}O_{68}(O,OH)_{10}$, a new species isostructural with vesuvianite, from the Sakha Republic, Russian Federation. Canadian Mineralogist, 36, 1301–1304.

Harley, S.L. (1998a) On the occurrence and characterization of ultrahigh-temperature crustal metamorphism. In P.J. Treloar and P.J. O'Brien, Eds., What Drives Metamorphism and Metamorphic reactions?, 138, 81–107. Geological Society of London Special Publications, U.K.

———(1998b) An appraisal of peak temperatures and thermal histories in ultrahigh-temperature (UHT) crustal metamorphism: the significance of aluminous orthopyroxene. In Motoyoshi, Y. and Shiraishi, K., Eds. Origin and Evolution of Continents, Memoirs NIPR, Special Issue, 53, 49–73. National Institute for Polar Research, Tokyo.

Harley, S.L. and Christy, A.G. (1995) Titanian 2:2:1 sapphirine in a partially melted aluminous granulite xenolith, Vestfold Hills, Antarctica: geological and mineralogical implications. European Journal of Mineralogy, 7, 637–653.

Hawthorne, F.C., Cooper, M., Bottazzi, P., Ottolini, L., Ercit, T.S., and Grew, E.S. (1995) Micro-analysis of minerals for boron by SREF, SIMS and EMPA: A comparative study. Canadian Mineralogist, 33, 389–397.

Higgins, J.B. and Ribbe, P.H. (1979) Sapphirine II: A neutron and X-ray diffraction study of $(Mg\text{-}Al)^{VI}$ and $(Al\text{-}Si)^{IV}$ ordering in monoclinic sapphirine. Contributions to Mineralogy and Petrology, 68: 357–368

Higgins, J.B., Ribbe, P.H., and Herd, R.K. (1979) Sapphirine I: Crystal chemical contributions. Contributions to Mineralogy and Petrology, 68: 349–356.

Hölscher, A. (1987) Experimentelle Untersuchungen im System MgO-BeO-Al_2O_3-SiO_2-H_2O: MgAl-Surinamite und Be-Einbau in Cordierit und Sapphirin. Unpublished Ph.D dissertation, Ruhr-Universität Bochum.

Hölscher, A. and Schreyer, W. (1989) A new synthetic hexagonal BeMg-cordierite, $Mg_2(Al_2BeSi_6O_{18})$, and its relation to Mg-cordierite. European Journal of Mineralogy, 1, 21–37.

Hölscher, A., Schreyer, W., and Lattard, D. (1986) High-pressure high-temperature stability of surinamite in the system MgO-BeO-Al_2O_3-SiO_2-H_2O. Contributions to Mineralogy and Petrology, 92, 113–127.

Jansen, J.B.H. (1977). Metamorphism on Naxos, Greece. Ph.D. Thesis, State University of Utrecht.

Kretz, R. (1983) Symbols for rock-forming minerals. American Mineralogist, 68, 277–279.

Lacroix, A. (1913) Minéralogie de la France et de ses colonies, Tome 5. Ch. Berenger, Paris.

Liu, T.C. and Presnall, D.C. (1990) Liquidus phase relations on the join anorthite-forsterite-quartz at 20 kbar with applications to basalt petrogenesis and igneous sapphirine. Contributions to Mineralogy and Petrology, 104, 735–742.

———(2000) Liquidus phase relations in the system CaO-MgO-Al_2O_3-SiO_2 at 2.0 GPa: application to basalt fractionation, eclogites and igneous sapphirine. Journal of Petrology, 41, 3–20.

Merlino, S. (1973) Polymorphism in sapphirine.Contributions to Mineralogy and Petrology, 41, 23–29.

Merlino, S. (1980) Crystal structure of sapphirine-1*Tc*. Zeitschrift für Kristallographie, 151, 91–100.

Merlino, S. and Pasero, M. (1987) Studio HRTEM della saffirina: relazioni tra politipi 1Tc e 2M e nuovo politipo 4M [in Italian] (abstract presented at meeting of La Società Italiana di Mineralogia e Petrologia, Pisa, Italy, May 1987).

Moore, P.B. (1969) The crystal structure of sapphirine. American Mineralogist, 54, 31–49.

———(1978) Welshite, $Ca_2Mg_4Fe^{3+}Sb^{5+}O_2[Si_4Be_2O_{18}]$, a new member of the aenigmatite group. Mineralogical Magazine, 42, 129–132.

Moore, P.B. and Araki, T. (1983) Surinamite, ca. $Mg_3Al_4Si_3BeO_{16}$: its crystal structure and relation to sapphirine, ca. $Mg_{2.8}Al_{7.2}Si_{1.2}O_{16}$. American Mineralogist, 68, 804–810.

Povondra, P. and Langer, K. (1971) Synthesis and some properties of sodium-beryllium-bearing cordierite $Na_xMg_2(Al_{4-x}Be_xSi_5O_{18})$. Neues Jahrbuch für Mineralogie Abhandlungen, 116, 1–19.

Sahama, Th.G., Lehtinen, M., Rehtijärvi, P., and von Knorring, O. (1974) Properties of sapphirine. Annales Academiae Scientarum Fennicae Series A III, 1–24.

Sandiford, M. and Powell, R. (1986) Pyroxene exsolution in granulites from Fyfe Hills, Enderby Land, Antarctica: Evidence for 1000 °C metamorphic temperatures in Archean continental crust. American Mineralogist, 71, 946–954.

Steffen, G., Seifert, F., and Amthauer, G. (1984) Ferric iron in sapphirine: a Mössbauer spectroscopic study. American Mineralogist, 69, 339–348.

Sutherland, F.L. and Coenraads, R.R. (1996) An unusual ruby-sapphire-sapphirine-spinel assemblage from the Tertiary Barrington volcanic province, New South Wales, Australia. Mineralogical Magazine, 60, 623–628.

Wilson, A.F. and Hudson, D.R. (1967) The discovery of beryllium-bearing sapphirine in the granulites of Musgrave Ranges (Central Australia). Chemical Geology, 2, 209–215.

MANUSCRIPT RECEIVED 12/27/2000
MANUSCRIPT ACCEPTED MARCH 28, 2002
MANUSCRIPT HANDLED BY JOHN C. SCHUMACHER